Doi: https://doi.org/10.54172/nkr1d641

Research Article 6 Open Access

Top Glass Cover Effect On The Performance of a Parabolic Trough Solar Receiver



Mohamed A. Eltarkawe^{1*}, Ali A.A. Adam² and Hasan A. H. Husayn³

*Corresponding author: mohamed.eltarkawe@omu.ly.edu, Department of Mechanical Engineering, Faculty of Engineering, Omar Al-Mukhtar University, Libya.

- ² Department of Mechanical Engineering, Faculty of Engineering, Omar Al-Mukhtar University, Libya.
- ³ Department of Renewable Energy Engineering, Faculty of Engineering, Omar Al-Mukhtar University, Libya

Received:

21 January 2024

Accepted:

19 November 2024

Publish online:

31 December 2024

Abstract

Solar energy is a promising solution to the rapidly increasing energy consumption. The parabolic trough collector (PTC) can be a practical solution, particularly in providing domestic water heating in developing countries. The impact of the glass envelope on PTC performance has been investigated extensively. However, only a few studies have investigated the effects of a flat-top glass cover. This study examines the impact of a top glass cover on the PTC performance by manufacturing two identical PTCs, one with a top glass cover and the other without a top cover. The topcovered collector showed a higher maximum absorber surface temperature (11%) and higher maximum water temperature (4%) than the temperatures of uncovered PTC. The results also showed that the theoretical efficiency was %56.9 and the experimental efficiency was %50.4. Installing the glass cover has led to a gain in theoretical thermal efficiency by 5% and in experimental thermal efficiency by 4%. The study recommends that future studies improve the reflecting mirrors and increase the size of the prototype.

Keywords: Parabolic Solar Collector; Solar Energy; Thermal Efficiency; Top-Glass Cover; Energy Balance.

INTRODUCTION

Due to the fast increase in population worldwide, energy consumption has significantly increased, leading to high emissions levels. In addition, these conventional sources of energy will become extinct soon (Islam et al., 2018). Finding and developing alternative sources of energy have become inevitable (Ibrahim, 2020; de Oliveira Siqueira et al., 2014). Among the different renewable energy sources, solar energy is a promising solution to many challenges (Tian & Zhao, 2013; Brooks, 2005). Thermal solar collectors provide practical solutions to many applications ranging from electricity production to hot water supply for domestic usage (Maree & Ismaeel, 2019).

Depending on the concentration ratios, solar collectors are often divided into two categories: non-concentrating collectors and concentrating collectors. In a non-concentrating collector, the intercepting area equals the collector's absorbing area, while a concentrating solar collector often has concave reflecting surfaces larger than the intercepting area. The concentrating collector



The Author(s) 2024. This article is distributed under the terms of the Creative Commons Attribution 4.0 International License (http://creativecommons.org/licenses/by/4.0/), which permits unrestricted use, distribution, and reproduction in any medium 'provided you give appropriate credit to the original author(s) and the source, provide a link to the Creative Commons license, and indicate if changes were made.

tors can be classified into two groups: point concentrating and line concentrating (Tian & Zhao, 2013; Fernández-García et al., 2010; Hachicha, 2013). Point-concentrating technologies focus solar radiation on a single point. The most common applications of this method are the dish/engine systems and central receiver systems (Hachicha, 2013). On the other hand, line concentration systems collect the incoming energy from the sun using long rectangular or curved mirrors. These mirrors reflect and concentrate the sunlight on tubes (or absorbers). A fluid flowing inside the tubes will then be heated and transferred to a storage or steam turbine generator to produce electricity. An example of a concentrating collector is the Parabolic trough collector (PTCs), which consists of a trough mirror that concentrates the incoming solar energy onto an absorber tube, which transports the energy to the working fluid passing inside it (Tian & Zhao, 2013; Fernández-García et al., 2010; Abed & Afgan, 2020; Ahmed et al., 2016).

The PTC systems have proven to be a feasible and promising technology for the future of renewable energy in many places around the world, including developing countries. The positive impact of a glass annulus envelope on the PTC performance is well-known and extensively investigated. However, glass annulus envelope technology increases the cost of the solar collector significantly. For the PTC technology to succeed particularly in developing countries, the cost must be reduced even with slightly compromising efficiency. Using a flat-top glass cover instead of a glass annulus envelope (Bhujangrao, 2015) will significantly reduce the manufacturing cost. Low-cost PTCs can be a practical solution to the energy challenge in Libya, which has been suffering from power outages and rolling blackouts due to the high demand and limited power production.

Only a few studies have investigated the impact of a flat-top-glass cover on PTC performance (Maree & Ismaeel, 2019; Ahmed et al., 2016). However, to our knowledge, none of the previous studies have compared the performance of a flat-top-glass-covered collector using two identical collectors working simultaneously on the same day. Bhujangrao used only one collector to take the measurements on two different days, which could affect the study results (Bhujangrao, 2015).

This work aims to investigate the effect of the top glass cover on the performance of a PTC prototype in Al-Bayda, Libya. This objective can be achieved by studying the temperature behavior of the absorber outer surface and heat transfer fluid of a covered and an uncovered PTC. The effect of the top cover on the thermal efficiency will also be investigated. The two identical parabolic solar collectors are run simultaneously with the same characteristics.

MATERIALS AND METHODS

Experimental work

Two identical prototype PTCs were designed and manufactured at the mechanical engineering laboratories at Omar Al-Mukhtar University. One of the PTCs was covered with a flat-top glass cover, and the other PTC was left without a glass cover (Figure 1). The parabola surface formula used for the designing and manufacturing of the reflecting surface is represented by equation (1) (Abed & Afgan, 2020; Ahmed et al., 2016; Price et al., 2002).

$$Y = \left(\frac{1}{4f}\right)X^2\tag{1}$$

Each PTC was made of a wood frame with an aperture area of 920 cm 2 (40 cm \times 23 cm). The reflectors were glass mirror strips (40 cm \times 2.5 cm) (Woodrow, 2016). The absorbers were made of

copper and had a 10 mm inside diameter and a 12 mm outside diameter. The heat transfer fluid used in both collectors was water flowing in a closed loop, from an iron tank to the collector and circulating back to the tank. Ambient temperature was measured using a liquid-in-glass thermometer, and the wind was measured using an Anemometer (TENMA 72-6638), while solar radiation was measured using a solar power meter (CEM- LA- 1017) in units of W/m². For the top covered collector, six thermocouples (k-type) were connected to the service unit, recording receiver inner and outer surface temperatures, and water temperatures at the inlet and outlet of the solar collector. The uncovered solar collector was connected to four thermocouples: receiver inner and outer surface and water temperatures at the inlet and outlet. To ensure that the flow rate in both collectors is the same, two identical internal liquid filter pumps (JY-600F) were used. At the beginning of the experiment, the flow rate was measured by dividing a collected volume in a bucket by the filling time to verify that the flow rate in both collectors was the same. All measuring devices used during the experimental work are detailed in Supplementary section S1, and all thermocouples, the service unit, the solar radiation meter, and the anemometer were calibrated at the beginning of this study.

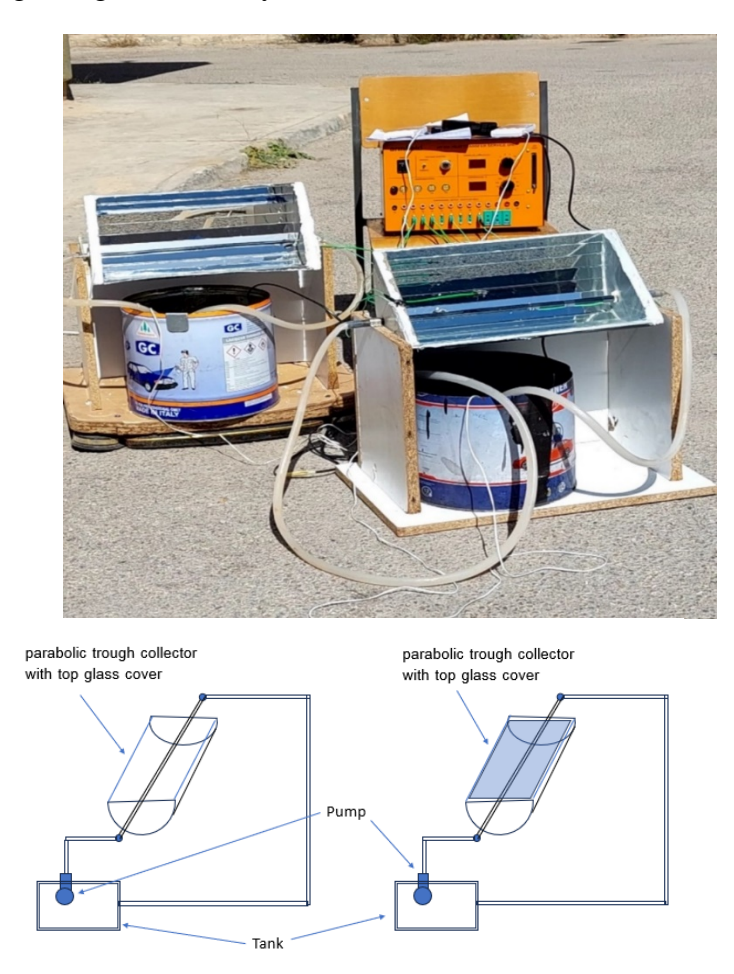


Figure: (1). Two identical PTC prototypes with and without a top glass cover during operation are shown schematically and in the testing setup.

One day was selected to conduct the measurements every month, preferably a blue-sky day. No measurements were taken for April because of the weather conditions. For the selected day, the tilt angle was calculated using equation (2), and the used MATLAB code is shown in supplementary C1 (Yadav & Chandel, 2013; Handoyo & Ichsani, 2013; Benghanem, 2011). More specifically, the

declination angle was first calculated based on the day number in the year, n. Secondly, since the collectors were oriented to the south, a zero-surface azimuth angle was used in calculations. The geographical latitude of 32.76272N (Al Bayda City) was used, and the hour angle was selected to be solar noon. As a result, the calculated tilt angle for both collectors will be identical and fixed for the entire day but change daily.

Both collectors were provided by protractors placed on the frame at the moving axis of the collector. The protractors give an accurate reading of the tilt angle for both collectors. After setting the collectors to the desired tilt and surface azimuth angle, measurements of receiver inner and outer surface temperatures, inner and outer glass cover surface temperatures, water temperatures at the inlet and outlet of the solar collector, wind speed, and solar radiation were recorded every 5 minutes. The volumetric flow rate was measured once in every experiment.

$$\tan \beta = \frac{(\cos \delta \sin \gamma \sin \omega - \sin \delta \cos \varphi \cos \gamma + \cos \delta \sin \varphi \cos \gamma \cos \omega)}{(\sin \delta \sin \varphi + \cos \delta \cos \varphi \cos \omega)}$$
(2)

where,

- β Tilt angle
- φ Latitude
- δ Declination angle
- γ Surface azimuth angle
- ω Hour angle
- γ Solar azimuth angle

Energy balance

Equilibrium energy equations have been used to compare inlet solar energy with outlet valuable energy reaching the water tank to investigate the top glass cover effect on the parabolic trough solar receiver performance. Figure 2 and Figure 3 show schemes of two parabolic solar collectors, one with a top glass cover and the other without a top glass cover. Similarly, Figure 4 and Figure 5 show the thermal resistance network of heat flow (Forristall, 2003; Qu et al., 2007; Gong et al., 2010).

When the top glass is attached, the solar energy (Q_i) reaches the solar collector and hits the top glass. Some of this energy passes to the receiver tube, defined as actual solar energy (Q_{act}) , while the rest of the energy is lost as optical losses. It is important to mention that the system is assumed to be in equilibrium, and all thermodynamic properties are uniformly distributed around the absorber. The optical losses are due to many factors, such as accumulating dust on the mirrors, blocking, and mirror reflectivity (Forristall, 2003).

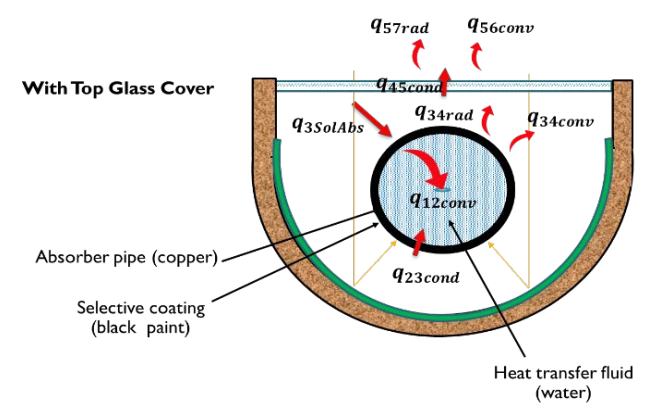


Figure: (2). Scheme of a parabolic solar collector covered with a top glass cover.

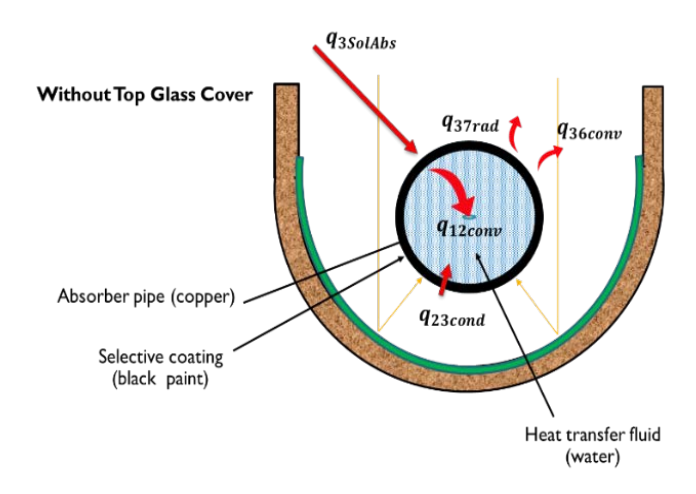


Figure: (3). Scheme of a parabolic solar collector without a top glass cover.

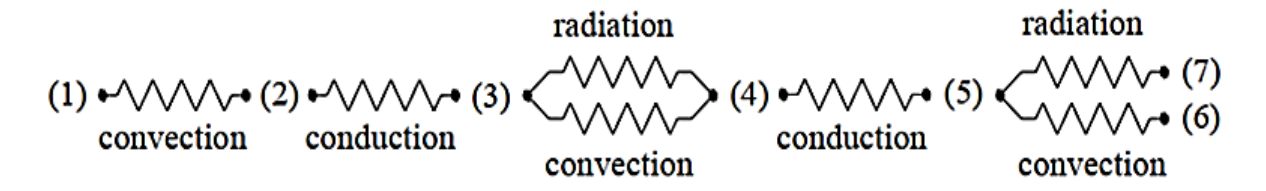


Figure: (4). Thermal resistance model of a 1-Dimension for a to glass covered parabolic solar collector.

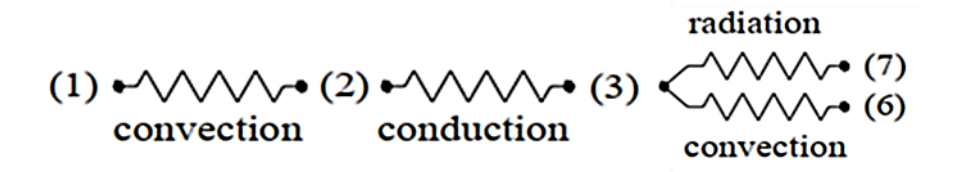


Figure: (5). Thermal resistance model of a 1- Dimension for a parabolic solar collector without a top glass cover

Solar collector with a top glass cover

In the case when the top glass cover is attached, the one-dimensional heat transfer equations are presented below (Brooks, 2005, Forristall, 2003):

| $Q_{12\text{convection}} = Q_{23\text{conduction}}$ | (3) |
|---|-----|
| $Q_{\text{act}} = Q_{34\text{convection}} + Q_{34\text{radiation}} + Q_{23\text{conduction}}$ | (4) |
| $Q_{34\text{convection}} + Q_{34\text{radiation}} = Q_{45\text{conduction}}$ | (5) |
| $Q_{45\text{conduction}} = Q_{56\text{convection}} + Q_{57\text{radiation}}$ | (6) |
| $Q_{Heatloss} = Q_{56convection} + Q_{57radiation}$ | (7) |

However, when no top glass cover is attached, the heat transfer model is reduced since the heat transfers from the receiver to the atmosphere directly:

$$\begin{aligned} Q_{12\text{convection}} &= Q_{23\text{conduction}} & (8) \\ Q_{act} &= Q_{36\text{convection}} + Q_{37\text{radiation}} + Q_{23\text{conduction}} & (9) \\ Q_{\text{Heatloss}} &= Q_{36\text{convection}} + Q_{37\text{radiation}} & (10) \end{aligned}$$

Convective heat from the tube to water

Heat is transferred from the inner surface of the receiver to the water via convection, as given by the following equation (Forristall, 2003):

$$Q_{12\text{convection}} = U_1 D_2 \pi (T_2 - T_1)$$

$$U_{1=} N_{uD_2} \frac{K_1}{D_2}$$
(12)

where,

 U_1 = Coefficient of convection heat transfer

 $D_2 = Receiver inner diameter$

 $K_1 =$ Water conductivity at T_1

 T_1 = Water average temperature

 T_2 = Inner surface temperature of the receiver

Nu_{D2}= Nusselt number based on inner diameter.

Based on the flow type (turbulent, transitional, or laminar), the model uses a suitable Nusselt number. In case of turbulent and transitional flow, the following equations are used to calculate the Nusselt number (de Oliveira Siqueira et al., 2014; Abed & Afgan, 2020; Forristall, 2003):

$$Nu_{D2} = \frac{\frac{Df_2}{_8(Re_{D2} - 1000)Pr_1}}{\frac{1}{_{1+12.7}\sqrt{\frac{Df_2}{_8}\left(Pr_1^{\frac{2}{3}} - 1\right)}} \left(\frac{Pr_1}{Pr_2}\right)^{0.11}}$$
(13)

$$Df_2 = (1.82 \log_{10}(Re_{D_2}) - 1.64)^{-2}$$
 (14)

where,

Df₂ = Darcy–Weisbach friction factor

Re_{D2}= Reynolds number

Pr₁ and Pr₂ = Prandtl number at the receiver's centerline and inner surface, respectively.

There are some important assumptions regarding the above equations. For example, the inner surface of the absorber is smooth, the turbulent range of the Reynolds number should be less than 5000000, and the Prandtl number, Pr_1 , range should be less than 2000 (Forristall, 2003). If the flow is laminar (Re < 2300), the Nusselt number will be selected as 4.4 (Forristall, 2003).

Heat conduction through the receiver tube

The heat conduction through the wall of the receiver tube can be calculated using the following equation (Forristall, 2003; Gong et al., 2010):

$$Q_{23\text{conduction}} = 2\pi K_{23} (T_2 - T_3) / \ln \left(\frac{D_3}{D_2} \right)$$
 (15)

where,

 K_{23} = Copper thermal conductivity.

 D_3 = Receiver outer diameter

 T_3 = Outer surface temperature of the receiver

The thermal conductivity of copper used in the calculation is 400 W/m-K (Forristall, 2003).

Heat flow from the receiver to the inner surface of the top glass cover

Heat loss from the absorber to the inner surface of the top glass cover is caused by convection and radiation. Due to the presence of the top glass, the convection will be considered natural heat transfer only. The radiation heat flow also happens between the receiver and the top glass cover because of the temperature difference.

Convection heat transfer from the receiver to the inside surface of the top glass cover

The convection heat moving from the receiver's outer surface to the top glass cover is given by the equation below:

$$Q_{34convection} = U_{34}D_3\pi(T_4 - T_3)$$
 (16)

$$U_{34} = N_{uD_3} \frac{K_{34}}{D_3} \tag{17}$$

where,

 U_{34} = Ceofficient of convection heat transferCoefficient of convection heat transfer

 K_{34} = Air thermal conductivity

 T_4 = Inner glass cover surface temperature

 N_{uD_3} = Nusselt number based on D_3 Nusselt number based on D_3

The following correlation can estimate the Nusselt number:

$$N_{uD_3} = \left(0.60 + \frac{0.387Ra_{D_3}^{1/6}}{\left(1 + \left(0.559/P_{r_34}\right)^{9/16}\right)^{8/27}}\right)^2$$
(18)

$$Ra_{D_3} = \frac{g\beta(T_4 - T_3)D_3^3}{\alpha_{34}v_{34}}$$
 (19)

$$\beta = \frac{1}{T_{2d}} \tag{20}$$

$$P_{r34} = \frac{v_{34}}{\alpha_{34}} \tag{21}$$

where.

 $Ra_{D_3} = Rayleigh no.$ for air based on D_3 .

 v_{34} = Kinematic viscosity for air at T_{34}

 β = Volumetric thermal expansion coeff.

g = Gravitational constant

 α_{34} = Thermal diffusivity for air at T_{34}

 P_{r34} = The prandtl number for air at T_{34} .

It is assumed that equation 16 is valid for Rayleigh numbers ranging from 500000 to 10^{12} (Forristall, 2003).

Radiation heat moving from the receiver to the inside surface of the top glass cover

The Radiation heat flow from the receiver to the top glass cover can be estimated by the equation below:

$$Q_{34\text{radiation}} = \sigma \pi \varepsilon_3 D_3 (T_3^4 - T_4^4)$$
 (22)

where.

 $\sigma = Stefan-Boltzmann constant$

 ε_3 = The absorber selective coating emissivity

Conduction heat transfer across the top cover

Equation (21) estimates the flow of heat through the glass cover thickness.

$$q_{45\text{conduction}} = K_{45} A \frac{(T_4 - T_5)}{\Delta x}$$
 (23)

where.

 K_{45} = Thermal conductance of glass at T_{45}

T5 = Outer glass cover surface temperature

 $\Delta x = Glass cover thickness$

A = Area of glass cover

Heat between the top glass cover and the atmosphere

The heat transferred from the outer surface of the top glass cover to the atmosphere is by convection and radiation. The convection will be forced if the wind blows on the top glass cover. If there is no wind, the convection will be natural (Forristall, 2003).

Convection heat transfer from the outer surface of the top glass cover to the atmosphere

Equation (22) is used to calculate the convection heat flow from the outside surface of the top glass cover to the the atmosphere as can be seen below:

$$q_{56\text{convection}} = UA(T_5 - T_6) \tag{24}$$

$$U = \frac{N_u K}{L} \tag{25}$$

 K_5 = Air thermal conductivity

 $T_6 = Ambient temperature$

L = Length of glass cover

U = Convection heat transfer coefficient

Convection heat transfer when wind is present

The presence of the wind forces convection on the top glass cover. The Nusselt number will mainly depend on the flow type:

For Laminar case

$$N_{\rm u} = \frac{hL}{K} = 0.332 R_{\rm e5}^{1/2} P_{\rm r5}^{1/3}$$
 (26)

For Turbulent case

$$N_{\rm u} = \frac{\rm hL}{\rm K} = {\rm P_{r5}}^{1/3} (0.037 {\rm R_{e5}}^{0.8} - 871) \tag{27}$$

 $Pr_5 = Prandtl$ number evaluated at T_5 .

 Re_{T_e} = The Reynolds number based on T_5 .

Convection heat transfer when no wind is present

When air is calm, the convection heat flow from the top cover to the atmosphere is considered free convection. In this case, the Nusselt number can be estimated via the following equation ($G_{r5}P_{r5}$ < 2×10^8):

$$N_{\rm u} = 0.13 (G_{\rm r5} P_{\rm r5})^{1/3} \tag{28}$$

 G_{r5} = The Grashof number based on T_5 .

Radiation heat transfer from the outside surface of the top glass cover to the surroundings

The radiation from the top cover to the atmosphere is calculated using the equation below:

$$Q_{57 \text{radiation}} = \sigma \varepsilon_5 A \left(T_5^4 - T_7^4 \right) \tag{29}$$

where.

 ε_5 = Absorber selective coating emissivity

 $T_7 = sky temperature$

It is important to mention that the sky temperature is calculated as eight degrees Celsius lower than the ambient temperature (Forristall, 2003).

Solar collector without glass cover

The convection and radiation heat transfer are lost directly to the environment without the glass cover. With no wind, the convection is considered natural, and the equations (14 to 19) will be used. If wind is present, the convection heat flow from the receiving tube to the atmosphere is considered forced convection. In this case, the Nusselt number is calculated using the equation below (Forristall, 2003):

$$\overline{N}_{u_{D3}} = A \operatorname{Re}_{D3}{}^{B} \operatorname{Pr}_{4}{}^{C} \left(\frac{\operatorname{Pr}_{4}}{\operatorname{Pr}_{3}}\right)^{1/4}$$
 (30)

where.

 P_{r3} and P_{r4} = The Prandtl number for air at T_3 and T_4 respectively

 Re_{D_3} = Reynolds no. for air based on D3

In equation (28), Reynolds number determines the variables A and B: For 1 < Re < 40, A = 0.75 and B = 0.4. For 40 < Re < 1000, A = 0.51 and B = 0.5. For 1000 < Re < 200000, A = 0.26 and B = 0.6. For 200000 < Re < 1000000, A = 0.076 and B = 0.7. The value depends on the Prandtl number. It is 0.37 when Prandtl equals or less than ten, and 0.36 when Prandtl is equal to or greater than 10.

Theoretical and Experimental Efficiency

The theoretical efficiency is the useful energy or heat gain ratio to the solar energy reaching the solar collector. The solar energy reaching the solar collector is calculated using the following equation (Abed & Afgan, 2020):

$$Q_i = I_b * A_{aperture}$$
 where,
 $I_b = Solar radiation$ (31)

A aperture = Area of the collector

Only a fraction of solar energy is received by the absorber. This fraction is called adequate solar energy. The rest of the solar energy is lost due to the optical efficiency of the collector, which depends on glass cover properties, mirror properties, and metal tube properties. Glass is not perfectly transparent, with some losses from reflection and absorption. The reflective losses depend on the incidence angle of the solar irradiation. Therefore, to understand the performance of a glass cover, it is essential to consider the following three valuable metrics: transmittance (τ) , reflectance (ρ) , and absorptance (α) . For more information about solar radiation measurements and data, see supplementary D1.

The equation for the adequate solar energy becomes:

$$Q_{act} = Q_i * \eta_{opt}$$
 (32)

where,

Qi = Solar energy

 η_{opt} = Optical efficiency

Theoretical heat gain is the effective solar energy minus the heat transfer losses. Therefore, the theoretical heat gain is calculated using the equations:

$$Q_{Gain} = Q_{act} - Q_{loss}$$
 (33)

$$Q_{loss} = Q_{34convection} + Q_{34radiation}$$
 (34)

where,

 Q_{loss} = Heat losses

 $Q_{34convection}$ = Convection heat transfer from the receiver to the inside surface of the top cover

 $Q_{34\text{radiation}} = \text{Radiation heat transfer from the receiver to the inside surface of the top cover}$

Finally, the theoretical efficiency can be estimated using the following equation (Abed & Afgan, 2020):

$$\eta_{\text{Theoretical}} = \frac{Q_{\text{Gain}}}{Q_{\text{i}}} \tag{35}$$

To calculate the experimental efficiency, the solar energy reaching the collector is estimated using the same equation (29)(Brooks, 2005; Abed & Afgan, 2020; Kalogirou & Panayiotou, 2013). The experimental heat gain is calculated using the following equation:

$$Q_{Gain} = \dot{m} * C_p * (T_{in} - T_{out})$$
 (36)

where.

 \dot{m} = The flow rate of mass

 T_{in} = Water temperature at the outlet

 $T_{out} = Water temperature at the inlet$

 $C_p = Water specific heat$

The experimental efficiency of the PTC is the ratio of the heat gained to the solar energy reached by the collector. The experimental efficiency is calculated using equation 38 (Brooks, 2005; Kalogirou & Panayiotou, 2013):

$$\eta_{Experimental} = \frac{Q_{Gain}}{Qi}$$
 (38)

RESULTS AND DISCUSSION

The water and absorber outside surface temperatures for the covered collectors

For the top-covered solar collector, measurements were taken during ten months in 2022, from February to December (except April). Figure 6 shows the water and absorber temperature change over time in February. See supplementary (S2) for water and absorber temperatures from March to December. In general, both water and absorber temperatures increased gradually with time. The absorber temperature was mainly higher than the water temperature.

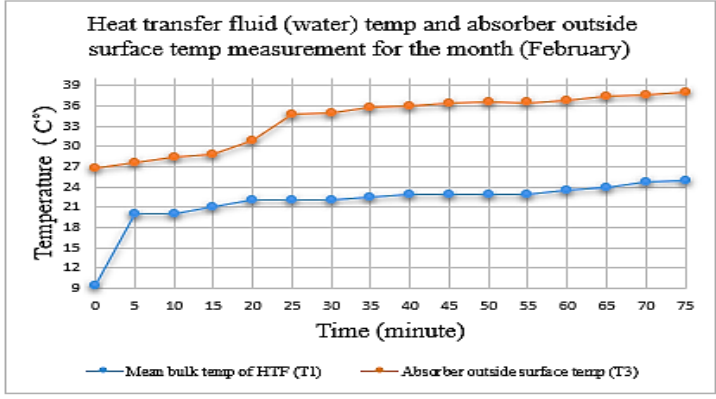


Figure: (6). Temperature of water and absorber outside surface during February.

The impact of top glass cover on absorber outside surface temperature and heat transfer temperature

The two identical solar collectors were run simultaneously during October, November, and December. Figure 7 shows the impact of top glass cover on absorber outside surface temperature during December. Both absorber surface temperatures increased with time, as expected, but the top-covered collector showed a more stable temperature increase, while the solar collector without a glass cover showed a fluctuating temperature increase. This is due to the impact of wind on the uncovered absorber. Supplementary S3 compares absorber outside surface temperatures of covered and uncovered PTCs for October and November.

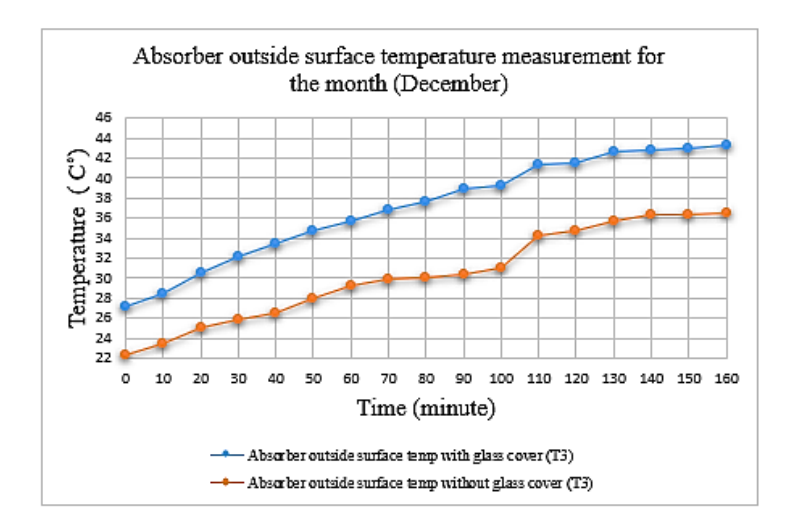


Figure: (7). Absorber outside surface temperature for the covered and uncovered collectors during December

Similarly, the top glass cover led to a higher water temperature than the uncovered PTC. Figure 8 shows the water temperature increase in a PTC with a top cover and an uncovered PTC during December. Similar comparisons for October and November are shown in the supplementary (S4).

The results showed that the top glass cover has a more significant effect on the absorber surface temperature than the water. The absorber surface temperature increased by 11%, while the water temperature increased by only 4% due to the presence of the top cover.

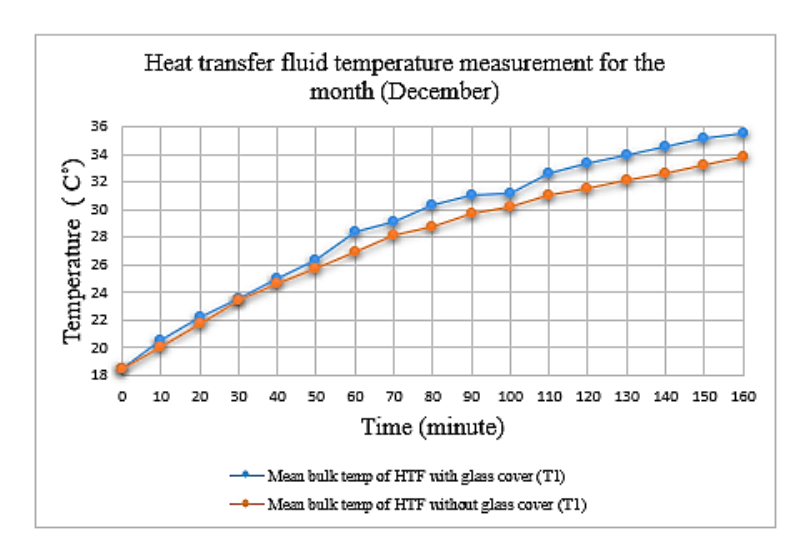


Figure: (8). Water temperature for the covered and uncovered collectors during December.

The results of the PTC thermal efficiency

Another important objective of this work is to investigate the effect of the top glass cover on the thermal efficiency of the parabolic solar collector. All parameters used in the efficiency calculations were during November 2022. Figure 9 compares the theoretical thermal efficiency of a covered and uncovered parabolic trough solar collector. The maximum theoretical thermal efficiency was 56.9%, and the maximum experimental efficiency was 50.4%. The theoretical thermal efficiency increases by 5% due to the presence of the top glass cover. The experimental thermal efficiency increased by less than 4% when the top cover was attached (Figure 10).

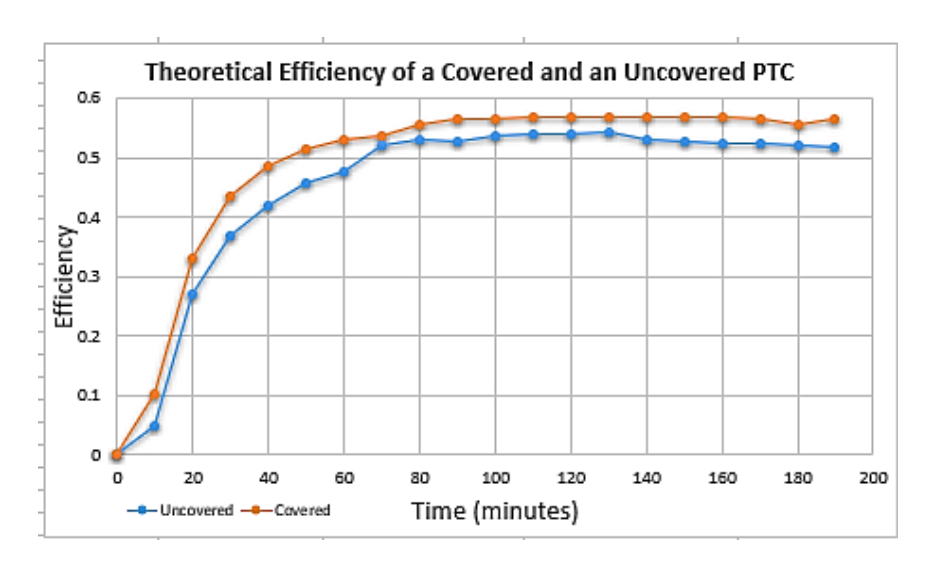


Figure: (9). Theoretical thermal efficiency of the covered and uncovered PTC

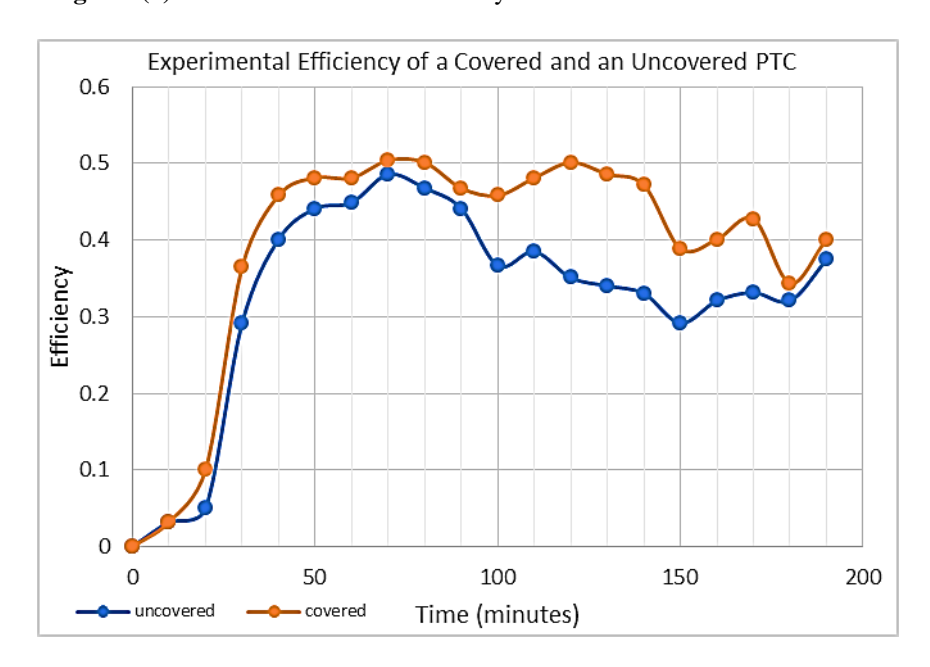


Figure: (10). Experimental thermal efficiency of the covered and uncovered PTC

Even though the temperature continuously increases with time, as shown in Figures 6,7, and 8, the theoretical thermal efficiency remains almost constant after about 80 minutes. Initially, the temperature is slightly low, meaning low heat loss. Therefore, the efficiency increases since the ratio of energy gained to available energy increases. On the other hand, as the temperature increases (after 80 minutes), the heat loss also increases, leading to a constant overall efficiency value. This is not en-

tirely unusual; several previous studies have reported a significant correlation between thermal efficiency and solar radiation, indicated by an increase before noon, which remains almost constant for a short period before it decreases when the solar radiation becomes weaker. Singh et al. (2012), who designed an aluminum-framed parabolic trough collector with a reflecting mirror (1.2 m \times 0.05 m), found that the efficiency increased until 10 am. It decreased until 1 pm. The maximum efficiency was relatively low (21%) (Singh et al., 2012).

The findings of this study about the maximum efficiency value are also consistent with previous studies. Brooks (2005) studied the performance of a PTC and found the maximum efficiency was 55.2% for an unshielded absorber (Brooks, 2005), Qu et al. (2006) reported that the maximum efficiency was 55% (Qu et al., 2007). Ahmed et al. (2016) found that the maximum efficiency of a PTC installed in Sabratha, Libya, was 43.9% (Ahmed et al., 2016). In Erbil, a city in Iraq, Maree and Ismaeel (2019) studied theoretical and experimental efficiency. They showed that the thermal efficiency decreased with time, and the maximum efficiency was pretty high (74%) (Maree & Ismaeel, 2019).

A closer look at Figure 10 shows a fluctuating decrease in the experimental thermal efficiency after about 80 minutes. There are a number of possibilities that could explain this unexpected behavior. Since thermal efficiency is strongly dependent on solar radiation, operating conditions, and optical losses, the efficiency decrease may be associated—in part—with the decrease in solar radiation that happened after 10:30 am (80 minutes) on Nov 10th, 2022 (please see supplementary D1 for the solar radiation data). However, this decrease does not explain the two drops at 100 and 150 minutes, which happened for covered and uncovered collectors, indicating that this was not due to the wind effect. These drops could be due to operation conditions such as laminar and turbulent flows.

CONCLUSION

The study aimed to design and manufacture two identical parabolic trough solar collectors with and without a top glass cover. The two collectors were manufactured and tested in the Mechanical Engineering Laboratories at the University of Omar Al-Mukhtar in Albayda, Libya. The effect of the top glass was studied, and the theoretical and experimental thermal efficiency of the solar collector was studied when the top glass was attached.

The results showed that both the absorber surface and the water temperatures gradually increased with time in both collectors. The top-covered collector showed a higher maximum absorber surface temperature (11%) and higher maximum water temperature (4%) than the temperatures of the uncovered collector. As expected, the absorber surface temperature was always higher than the water temperature.

The thermal efficiency comparison was conducted in November 2022. Installing the top-glass cover led to a gain in theoretical thermal efficiency by 5% and in experimental thermal efficiency by 4%. The results also showed that the maximum theoretical efficiency was 56.9%, and the maximum experimental efficiency was 50.4%. The efficiency values obtained in this study were consistent with many lab-manufactured PTCs but lower than some commercial PTCs. The findings provided in this study are crucial in providing a cost-effective PTC that can be an alternative energy source, especially in developing countries such as Libya. We recommend that future studies improve the reflecting mirrors and increase the size of the prototype. To reduce the experimental cost of the improved design, it is recommended that the collector efficiency or the output temperature is predicted using either statistical modeling or independent variables from artificial neural networks such as solar radiation, input temperature, and ambient temperature.

ACKNOWLEDGEMENT

The authors would like to thank the Mechanical Engineering Department at Omar Al-Mukhtar University for supporting the project. The authors thank Mr. Fadeel Al-Areeda for lending the solar power meter.

Duality of interest: The authors declare that they have no duality of interest associated with this manuscript.

Author contributions: Hasan A. H. Husayn: performed, Conceptualization, Methodology, Software, Validation, Formal analysis, Resources, Data curation, Writing – original draft, review and editing. Mohamed Eltarkawe: performed, Conceptualization, Methodology, Writing – review & editing, Supervision, Project administration.

Funding: No specific funding was received for this work.

REFERENCES

- Abed, N., & Afgan, I. (2020). An extensive review of various technologies for enhancing the thermal and optical performances of parabolic trough collectors. *International Journal of Energy Research*, 44(7), 5117-5164.
- Ahmed, A. M., Albusefi, A. A., & Izweik, H. T. (2016). Experimental Evaluation of a Solar Parabolic Trough Collector under Libyan climate. *Int. J. Eng. Trends Technol*, 38(1), 32.
- Benghanem, M. J. A. E. (2011). Optimization of tilt angle for solar panel: Case study for Madinah, Saudi Arabia. *Applied Energy*, 88(4), 1427-1433.
- Bhujangrao, K. H. (2015). Effect of top glass cover on thermal performance of cylindrical parabolic collector. *International Research Journal of Engineering and Technology*, 2(8), 2015.
- Brooks, M. J. (2005). *Performance of a parabolic trough solar collector* (Doctoral dissertation, Stellenbosch: University of Stellenbosch).
- de Oliveira Siqueira, A. M., Gomes, P. E. N., Torrezani, L., Lucas, E. O., & da Cruz Pereira, G. M. (2014). Heat transfer analysis and modeling of a parabolic trough solar collector: an analysis. Energy Procedia, 57, 401-410.
- Fernández-García, A., Zarza, E., Valenzuela, L., & Pérez, M. (2010). Parabolic-trough solar collectors and their applications. *Renewable and sustainable energy reviews*, 14(7), 1695-1721.
- Forristall, R. (2003). *Heat transfer analysis and modeling of a parabolic trough solar receiver implemented in engineering equation solver* (No. NREL/TP-550-34169). National Renewable Energy Lab.(NREL), Golden, CO (United States).
- Gong, G., Huang, X., Wang, J., & Hao, M. (2010). An optimized model and test of the China's first high temperature parabolic trough solar receiver. *Solar Energy*, 84(12), 2230-2245.
- Hachicha, A. A. (2013). Numerical modelling of a parabolic trough solar collector.

- Handoyo, E. A., & Ichsani, D. (2013). The optimal tilt angle of a solar collector. *Energy Procedia*, 32, 166-175.
- Ibrahim, I. D. (2020). Development of Smart Parabolic Trough Solar Collector for Water Heating and Hybrid Polymeric Composite Water Storage Tank. *Université Paris-Saclay; Tshwane University of Technology*.
- Islam, M. T., Huda, N., Abdullah, A., and Saidur, R. (2018). A comprehensive review of state-of-the-art concentrating solar power (CSP) technologies: Current status and research trends. *Renewable and Sustainable Energy Reviews*, 91, 987-1018.
- Kalogirou, S. A., & Panayiotou, G. (2013). Experimental investigation of the performance of a Parabolic Trough Collector (PTC) installed in Cyprus. *In 2nd Conference on Power Options for the Eastern Mediterranean Region*.
- Maree, I. E., & Ismaeel, A. G. (2019). Experimental and theoretical calculation of efficiency for flat plate solar collectors in Erbil City. *Periodicals of Engineering and Natural Sciences*, 7(2), 786-793.
- Price, H., Lu" pfert, E., Kearney, D., Zarza, E., Cohen, G., Gee, R., & Mahoney, R. (2002). Advances in parabolic trough solar power technology. *J. Sol. Energy Eng.*, 124(2), 109-125.
- Qu, M., Archer, D. H., & Yin, H. (2007, January). A linear parabolic trough solar collector performance model. In *Energy Sustainability* (Vol. 47977, pp. 663-670).
- Singh, S. K., Singh, A. K., & Yadav, S. K. (2012). Design and fabrication of parabolic trough solar water heater for hot water generation. *International Journal of Engineering Research & Technology (IJERT)*, 1(10), 1-9.
- Tian, Y., & Zhao, C. Y. (2013). A review of solar collectors and thermal energy storage in solar thermal applications. Applied energy, 104, 538-553.
- Woodrow, O. R. (2016). Characterisation of a Parabolic Trough Collector Using Sheet Metal and Glass Mirror Strips. University of Pretoria (South Africa).
- Yadav, A. K., & Chandel, S. S. (2013). Tilt angle optimization to maximize incident solar radiation: A review. *Renewable and sustainable energy reviews*, 23, 503-513.